The 2007 Europhysics Conference on High Energy Physics IOP Publishing
Journal of Physics: Conference Series **110** (2008) 092027 doi:10.1088/1742-6596/110/9/092027

First CALICE results from test-beam data

Sebastian Schätzel[1]
DESY, Notkestr. 85, D-22607 Hamburg, Germany
E-mail: Sebastian.Schaetzel@desy.de

Abstract. Highly granular calorimeters are mandatory in the particle flow concept for ILC detectors. The CALICE Collaboration has built prototypes of finely segmented electromagnetic and hadronic calorimeters and operated them in beam tests in 2006. First analyses reproduce known physics results and the performance of the detectors is close to expectations from Monte Carlo simulations. Tracks have been reconstructed inside the electromagnetic calorimeter. The measured data will be used in future analyses to test and improve particle flow algorithms and shower models.

1. Introduction

In ILC detectors based on the particle flow concept, the tracking momentum resolution is better than the calorimeter energy resolution for most of the produced charged particles (i.e., up to single particle energies $\approx$ 100 GeV). Jets can be measured to a precision of $30\%/\sqrt{E/\mathrm{GeV}}$ in such a detector [1] by measuring all charged particles with the tracker and using the calorimeters to measure only the neutral particles. To avoid double-counting, calorimeter clusters initiated by charged particles must be separated from entries made by neutral particles. This can be achieved offline by topological algorithms provided that the calorimeter cells are small enough. The CALICE Collaboration has built prototypes of such calorimeters and operated some of them in test beams in 2006 with the aim to establish the technology which allows these high granularities and to study the fine structures of particle showers to benchmark and improve existing shower models and reconstruction algorithms.

2. Silicon-tungsten electromagnetic calorimeter (ECAL)

The ECAL used in the beam test is a silicon-tungsten sandwich type calorimeter with an analogue read-out using silicon diode wafers segmented into 1x1 cm^2 pads. The active layers are placed inside a frame structure (36x36 cm^2 surface, 20 cm depth) made of tungsten sheets which are wrapped in carbon fibre. The ECAL consists of 30 sandwich layers, corresponding to a total of 6480 channels and 24 radiation lengths.

3. Scintillator-steel hadronic calorimeter (HCAL)

A scintillator-steel sandwich structure is employed in the beam test to measure hadrons. Polystyrene scintillator tiles of 0.5 cm thickness are used, read-out through a silicon photomultiplier (SiPM) which is embedded in one corner of the tile. 3x3 cm^2 tiles are used in the central core, surrounded by 6x6 and 12x12 cm^2 tiles for an active area of 1x1 m^2 per

[1] for the CALICE Collaboration

plane. The active layers are placed between 2 cm thick steel plates and 38 sandwich layers are foreseen in total, corresponding to 7632 channels. In August (October) 2006, only 15 (23) layers were instrumented.

The SiPM is a pixel matrix of photo diodes which are operated in Geiger mode. The pixel recharge time leads to a non-linear response of the SiPM to large signals which is corrected offline using calibration curves that have been measured individually for every SiPM in a controlled laboratory setup. The SiPM signal and gain depend on temperature by $\approx -4\%/\mathrm{K}$ and $\approx -2\%/\mathrm{K}$, respectively.

4. Results

4.1. ECAL linearity and energy resolution

The energy response of the ECAL was found to be linear within $\pm 1\%$ for incident electron energies in the range $1 - 50$ GeV. The energy resolution is shown in Figure 1. A fit yields $\Delta E/E = \frac{17.1(1)\%}{\sqrt{E/\mathrm{GeV}}} \oplus 0.5(1)\%$.[2] The resolution predicted by a Monte Carlo simulation based on GEANT4 is better by a factor ≈ 1.02 on average.

4.2. Tracks in the ECAL

From the shower centre-of-gravities $(\frac{\sum_i E_i x_i}{\sum_i E_i}, \frac{\sum_i E_i y_i}{\sum_i E_i})$ in every layer of the ECAL, tracks are reconstructed and compared to reference tracks from four drift chambers in front of the ECAL to determine the ECAL tracking resolution. The resolutions of the horizontal (x) and vertical (y) positions of the track on the first ECAL layer are shown in Figure 2 as a function of the beam energy. The resolution at 6 GeV is 2.61(3) mm for unstaggered ECAL cells. The cells were staggered in x which improved the resolution by ≈ 0.7 mm to a precision only approximately three times worse than that of the drift chambers. Also shown in the figure are expectations from Monte Carlo simulations which are in good agreement with the measurements. The resolutions of the track angles $\arctan(dx/dz)$ and $\arctan(dy/dz)$, in which z is the direction along the beam line, are found to be ≈ 35 mrad at 6 GeV, approximately a factor 10 worse than that of the drift chambers.

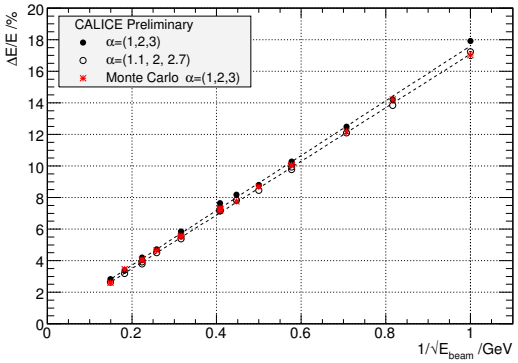

Figure 1. Relative energy resolution of the ECAL for electrons of energy E as a function of $1/\sqrt{E/\mathrm{GeV}}$.

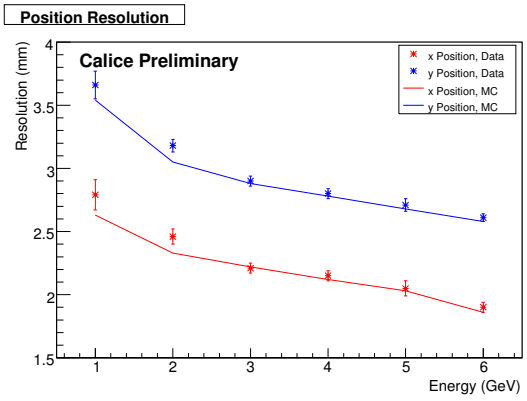

Figure 2. Position resolution for tracks reconstructed in the ECAL.

[2] The number in parentheses denotes the uncertainty of the last digit.

4.3. HCAL linearity and energy resolution

The response of the HCAL prototype to pions with energies in the range of $6-20$ GeV is shown in Figure 3 with the red square symbols corresponding to the measurements. For these energies the SiPM non-linearity exceeds 10% in less than 3% of the hit cells. After SiPM correction, the HCAL response is linear within a 2.5% systematic uncertainty which was deduced from a study of the response to muons which make up $10-20$% of the pion data sample, depending on energy. The uncertainty includes the effect of a day-to-night temperature variation of ≈ 1 K which was not corrected for.

The HCAL energy resolution is found to be described by $\Delta E/E = \frac{64(1)\%}{\sqrt{E/\mathrm{GeV}}} \oplus 8(1)\%$ but suffers from the partial instrumentation and shower leakage. For contained showers, which are selected by a veto on the signal recorded in a tail catcher detector behind the HCAL, the resolution is improved to $\approx 60\%/\sqrt{E/\mathrm{GeV}}$ with a vanishing constant term.

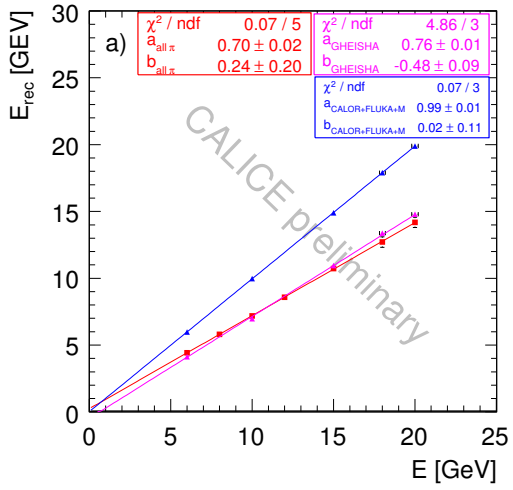

Figure 3. Energy response of the HCAL to pions as a function of the pion energy. The measurements are shown as the red square symbols. Also shown are predictions of two Monte Carlo simulations.

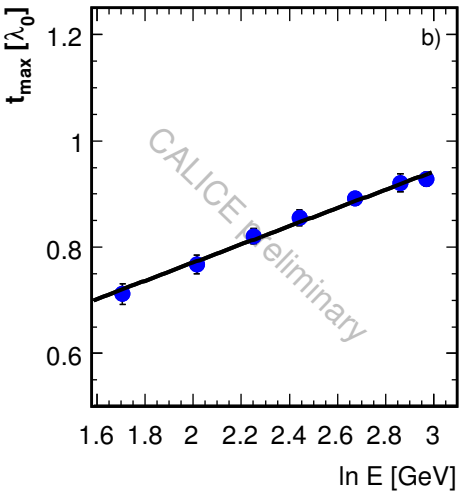

Figure 4. Depth of the maximum energy deposit in the HCAL as a function of $\ln(E/\mathrm{GeV})$.

4.4. Longitudinal hadronic shower profile

The longitudinal profile of pion showers in the HCAL follows the well-known form $dE/dt \propto t^a\, e^{-bt}$ in which t is the shower depth. The expected linear dependence of the depth $t_{\max}$ of the maximal energy deposition on the logarithm of the incident particle energy is found (Figure 4).

5. Conclusion

Prototypes of finely segmented electromagnetic and hadronic calorimeters at the ILC have been operated successfully in test beams. First analyses reproduce known physics results and the performance of the detectors is close to expectations from Monte Carlo simulations. Tracks have been reconstructed inside the electromagnetic calorimeter. The measured data will be used in future analyses to test and improve particle flow algorithms and shower models.

References

[1] Thomson M, these proceedings.